Limit Cycles in Piecewise Smooth Van der Pol Equations*

Zhihao Cen[1] and Feng Xie[1,†]

Abstract This paper focuses on analyzing the properties of equilibrium points and limit cycles in two types of planar piecewise smooth slow-fast systems. The right-half system is a classical van der Pol equation, while the left-half system is either linear or quadratic. Additionally, we provide a detailed description of the characteristics of limit cycles in these systems.

Keywords Limit cycles, slow-fast systems, van der Pol equations

MSC(2010) 34C07, 34C25, 34D15, 34E17.

1. Introduction

Van der Pol equations are a type of nonlinear differential equations that describe the behavior of oscillatory systems. The general form of van der Pol equation is modeled by a second-order differential equation

$$\frac{d^2x}{dt^2} - \mu(1-x^2)\frac{dx}{dt} + x = 0,$$

where x is the position of the oscillator, t is time, and μ is a parameter that controls the strength of the damping and the nonlinearity of the system [1]. It has been used to model a wide range of physical phenomena, including electrical circuits, chemical reactions, and biological systems.

One of the most interesting features of the van der Pol equation is its ability to exhibit limit cycle behavior. There are many results on the existence, stability and uniqueness of limit cycles for smooth Liénard systems [2]. In recent years, stimulated by nonsmooth phenomena in the real world, the relevant research has been extended to nonsmooth case, see for instance [3–6].

Recently, there has been a growing interest in the study of canard phenomena in nonsmooth systems. Recall that a canard is a trajectory of singularly perturbed differential equation that follows both the attracting and repelling slow manifolds for $O(1)$ time. Canard is associated with a bifurcation phenomena, named canard explosion, i.e. a transition from small Hopf cycles to relaxation oscillations through a sequence of canard cycles. It was first discovered in the context of the van der Pol oscillator with constant forcing and has important implications in applications,

we direct the reader to the paper by Benoit [7]. During the past few years, the focus of research has been on piecewise linear (PWL) systems. Desroches et al. [8] summarized the similarities and differences between PWL systems with three zones and smooth van der Pol system. For more studies in PWL canard phenomena, see for instance [9–11]. Andrew and Glendining turned their attention to piecewise smooth (PWS) Liénard systems, and they investigated the canard-like phenomena in PWS van der Pol systems [12] and extended the results in more general cases [13]. We remark that the above research mainly focuses on the existence of canard cycles. However, the asymptotic expansion of the parameter for which canard exists has not been provided.

In this paper we focus our attention on the existence of limit cycles and canard explosion. We consider two types of piecewise smooth van der Pol systems

$$
\dot{x} = -y + F(x), \quad F(x) = \begin{cases} (-1)^m k x^m, & x < 0, \\ x^2 - \frac{1}{3} x^3, & x \geqslant 0, \end{cases} \tag{1.1}
$$
$$
\varepsilon \dot{y} = (x - \lambda),
$$

where $k > 0$, $0 < \varepsilon \ll 1$, $m = 1$(or 2), and the dot denotes the derivative of x and y with respect to the time t. The set $S = \{(x,y) : y = F(x)\}$, called the critical manifold, plays a central role in the analysis of slow-fast system (1.1).

The structure of this paper is as follows: Section 2 examines the stability of equilibrium points and limit cycles for two types of van der Pol equations. Section 3 explores the impact of parameters on the limit cycle. The paper concludes with a discussion in Section 4.

2. Piecewise smooth van der Pol equations

2.1. Van der Pol equations with linear left branch

Considering the first type of piecewise smooth systems

$$
x' = -y + F_1(x), \quad F_1(x) = \begin{cases} -kx, & x < 0, \\ x^2 - \frac{1}{3} x^3, & x \geqslant 0, \end{cases} \tag{2.1}
$$
$$
y' = \varepsilon(x - \lambda),
$$

where $0 < \varepsilon \ll 1$, $k^2 - 4\varepsilon > 0$. It is clear that system (2.1) has a unique equilibrium point $E(\lambda, k\lambda)$ when $\lambda < 0$, or $E(\lambda, \lambda^2 - \frac{1}{3}\lambda^3)$ when $\lambda \geqslant 0$. For the convenience of discussion, we divide the plane into three regions as follows:

$$
L = \{(x,y)|x < 0\}, \quad M = \{(x,y)|0 \leqslant x \leqslant 2\}, \quad R = \{(x,y)|x > 2\}.
$$

2.1.1. The stability of the equilibrium point of system (2.1)

Theorem 2.1. *Let $\Delta = (2\lambda - \lambda^2)^2 - 4\varepsilon$. The stability of the equilibrium point E of system (2.1) is as follows.*

(1) *If $\lambda < 0$, then E is a stable node.*

(2) *If $\lambda = 0$, then E is a stable node in the left half-plane and a stable first-order focus in the right half-plane.*

(3) *If $0 < \lambda < 2, \Delta < 0$, then E is an unstable focus.*

(4) *If $0 < \lambda < 2, \Delta = 0$, then E is an unstable degenerate node.*

(5) *If $0 < \lambda < 2, \Delta > 0$, then E is an unstable node.*

(6) *If $\lambda = 2$, then E is a stable first-order focus.*

(7) *If $\lambda > 2, \Delta < 0$, then E is a stable focus.*

(8) *If $\lambda > 2, \Delta = 0$, then E is a stable degenerate node.*

(9) *If $\lambda > 2, \Delta > 0$, then E is a stable node.*

Proof. By simple calculation, we obtain that the Jacobian matrix of system (2.1) at the equilibrium point E is $\begin{pmatrix} -k & -1 \\ \varepsilon & 0 \end{pmatrix}$ for $\lambda < 0$ with its eigenvalues $\lambda_{1,2} = \frac{-k \pm \sqrt{k^2 - 4\varepsilon}}{2}$, and the Jacobian matrix is $\begin{pmatrix} \lambda - \lambda^2 & -1 \\ \varepsilon & 0 \end{pmatrix}$ for $\lambda \geqslant 0$ with its eigenvalues $\lambda_{1,2} = \frac{2\lambda - \lambda^2 \pm \sqrt{\Delta}}{2}$. Conculusions (1), (3)-(5) and (7)-(9) can be directly determined. For case (2), by the following coordinate and time scale transformations

$$\begin{cases} \bar{x} = \lambda - x, \\ \bar{y} = \varepsilon^{-\frac{1}{2}}(y - \lambda^2 + \frac{1}{3}\lambda^3), \\ \bar{t} = \varepsilon^{\frac{3}{2}}t, \end{cases}$$

the right-half system (2.1) is turned into a Liénard system

$$\begin{aligned} \frac{d\bar{x}}{d\bar{t}} &= \bar{y} + \frac{2\lambda - \lambda^2}{\sqrt{\varepsilon}}\bar{x} + \frac{\lambda - 1}{\sqrt{\varepsilon}}\bar{x}^2 - \frac{1}{3\sqrt{\varepsilon}}\bar{x}^3, \\ \frac{d\bar{y}}{d\bar{t}} &= -\bar{x}. \end{aligned} \tag{2.2}$$

For simplicity, we denote the variables $\bar{x}, \bar{y}, \bar{t}$ as x, y, t respectively. In this case, system (2.2) becomes

$$\begin{aligned} \frac{dx}{dt} &= y - \frac{1}{\sqrt{\varepsilon}}x^2 - \frac{1}{3\sqrt{\varepsilon}}x^3, \\ \frac{dy}{dt} &= -x. \end{aligned} \tag{2.3}$$

Choosing a locally positive definite function within a small neighborhood of the origin

$$V(x, y) = x^2 + y^2 - \frac{2}{\sqrt{\varepsilon}}x^2 y - \frac{4}{3\sqrt{\varepsilon}}y^3 - \frac{5}{12\sqrt{\varepsilon}}x^4 + \frac{4}{\varepsilon}x^3 y + \frac{1}{2\sqrt{\varepsilon}}x^2 y^2 + \frac{1}{4\sqrt{\varepsilon}}y^4.$$

Taking the derivative of V along the solutions of (2.3), we obtain

$$\frac{dV}{dt} = -\frac{1}{4\sqrt{\varepsilon}}(x^2 + y^2)^2 + o((x^2 + y^2)^2).$$

According to Liapunov's stability theory, we know that the zero solution is asymptotically stable, and therefore the equilibrium point is a stable focus. The proof of case (6) is similar. $\qquad\square$

2.1.2. Limit cycles of system (2.1)

Theorem 2.2. *There exists $\varepsilon_0 > 0$ such that for $0 < \varepsilon \leqslant \varepsilon_0$, the following statements hold for system* (2.1):

(1) *when $\lambda \leqslant 0$ or $\lambda \geqslant 2$, there is no limit cycle;*

(2) *when $0 < \lambda < 2$, there exists a unique stable limit cycle.*

Proof.   When $\lambda \leqslant 0$, the equilibrium point $E(\lambda, -k\lambda)$ is located inside the region L. The dynamical properties within region L are determined by the left-half system

$$
\begin{aligned}
x' &= -y - kx, \\
y' &= \varepsilon(x - \lambda).
\end{aligned}
\tag{2.4}
$$

System (2.4) has two invariant lines given by

$$
y + \lambda = \frac{-k \pm \sqrt{k^2 - 4\varepsilon}}{2}(x - \lambda), \quad x \leqslant 0.
$$

Therefore, we can conclude that system (2.1) does not have a limit cycle.

When $0 < \lambda < 2$, the equilibrium point $E(\lambda, \lambda^2 - \frac{1}{3}\lambda^3)$ is located inside the region M. We construct a boundary as follows.

$$
\begin{aligned}
l_1 &= \{(x, y) : y + \lambda = \tfrac{-k - \sqrt{k^2 - 4\varepsilon}}{2}(x - \lambda), \hat{x} \leq x \leq \lambda\}, \\
l_2 &= \{(x, y_1) : y_1 = -\lambda, \lambda \leq x \leq x_2 = (h^{-1}(y_1) + 1)\}, \\
l_3 &= \{(x_2, y) : y_1 < y < y_3 = h(2)\}, \\
l_4 &= \{(x, y) : y = m_4(x - x_2) + y_3, \lambda \leq x \leq x_2\}, \\
l_5 &= \{(x, y_5) : y_5 = m_4(\lambda - x_2) + y_3, \hat{x} < x < \lambda\}, \\
l_6 &= \{(\hat{x}, y) : y_6 < y < y_5, y_6 = \tfrac{-k - \sqrt{k^2 - 4\varepsilon}}{2}(\hat{x} - \lambda) - \lambda\},
\end{aligned}
$$

where $y_5 + \lambda = \frac{-k - \sqrt{k^2 - 4\varepsilon}}{2}(\hat{x} - \lambda)$, $h(x) = x^2 - \frac{1}{3}x^3$, $\hat{x} < -1$. We demonstrate that
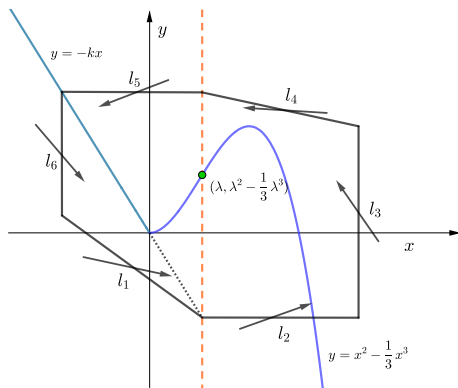
Figure 1. Boundary curves   **Figure 2.** Schematic diagram of limit cycle
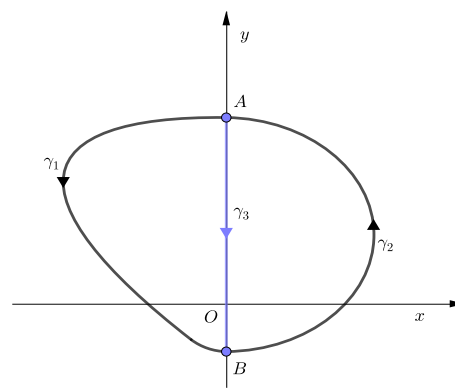
trajectories originating from any point on the boundary move towards the interior.

The slope of the tangent line to the trajectory passing through point $(x, y) \in l_4$ is given by

$$\frac{dy}{dx} = \frac{\varepsilon(x - \lambda)}{-y + x^2 - \frac{1}{3}x^3} = \frac{\varepsilon(x - \lambda)}{m_4(x - x_2) + y_3 + x^2 - \frac{1}{3}x^3},$$

where λ, m_4, x_2 and y_3 are constants. It is known that as $\varepsilon \to 0$, $\frac{dy}{dx} \to 0$ for $\lambda \leq x \leq x_2$}. Consider the set

$$\left\{(x, \varepsilon_x) : \left.\frac{dy}{dx}\right|_x > m_1, 0 < \varepsilon < \varepsilon_x\right\}.$$

By the continuity of the function, we can find a neighborhood $\bigcup(x, \delta_x)$ around x such that

$$\left.\frac{dy}{dx}\right|_{x_0} > m_4, \quad x_0 \in \bigcup(x, \delta_x), \quad 0 < \varepsilon < \varepsilon_x.$$

Therefore, we can construct an open cover $\{\bigcup(x, \delta_x) | \lambda \leqslant x \leqslant x_2\}$ for the closed interval $[\lambda, x_2]$. Applying the Heine-Borel theorem, we can obtain a finite open cover $\bigcup(x_i, \delta_{x_i})$, $i = 1, 2, \ldots, k$, such that

$$[\hat{x}, \lambda] \subseteq \bigcup_{i=1}^{k}(x_i, \delta_{x_i}).$$

We can choose ε_0 as the minimum value among $\varepsilon_{x_1}, \varepsilon_{x_2}, \ldots, \varepsilon_{x_k}$. With this choice, the proof is complete. Additionally, as we know that the equilibrium point is unstable, we can apply the Poincaré-Bendixon theorem to conclude that system (2.1) has at least one limit cycle. For the application of Poincaré-Bendixon theorem in piecewise smooth systems, please refer to [4, 10, 12, 13]. Now we prove that limit cycle must be stable and therefore unique.

Case 1: Assume that the limit cycle is located in region $L \cup M$ or $L \cup M \cup R$. When ε is sufficiently small, we calculate

$$\begin{aligned}
&\int_0^{T_1} \left(\frac{\partial P}{\partial x} + \frac{\partial Q}{\partial y}\right) dt + \int_{T_1}^{T_1+T_2} \left(\frac{\partial \tilde{P}}{\partial x} + \frac{\partial \tilde{Q}}{\partial y}\right) dt \\
&= \int_0^{T_1} -k dt + \int_{T_1}^{T_1+T_2} 2x - x^2 dt \\
&= \int_0^{T_1} -k dt + \int_{\gamma_2+\gamma_3} \frac{2x - x^2}{\varepsilon(x - \lambda)} dy - \int_{\gamma_3} \frac{2x - x^2}{\varepsilon(x - \lambda)} dy \\
&= \int_0^{T_1} -k dt + \int_O \frac{2x - x^2}{\varepsilon(x - \lambda)} dy < 0.
\end{aligned} \tag{2.5}$$

Thus, the limit cycle is stable and the result is proved. $T_1 + T_2$ is the period of the limit cycle, T_1 (T_2) is the time required for point A (B) to move to point B (A), and O is the closed curve $\gamma_2 + \gamma_3$.

Case 2: Assume that the limit cycle is located in region $M \cup R$. In this case, the dynamic properties of limit cycles are determined by the right-half system (2.1) and it has been proven to be stable.

When $\lambda \geqslant 2$, if there exists a limit cycle for system (2.1), it follows from equation (2.5) that the limit cycle is unique and stable. However, since the equilibrium point is stable, a contradiction arises.   □

Remark 2.1. The limit cycle of system (2.1) does not lie within a single region.

2.2. Van der Pol equations with parabolic-like left branch

Considering the second type of piecewise smooth systems

$$
\begin{aligned}
x' &= -y + F_2(x), \\
y' &= \varepsilon(x - \lambda),
\end{aligned}
\qquad
F_1(x) =
\begin{cases}
kx^2, & x < 0, \\
x^2 - \frac{1}{3}x^3, & x \geqslant 0,
\end{cases}
\tag{2.6}
$$

where $0 < \varepsilon \ll 1$ and $k > 0$. It is easy to see that system (2.6) has a unique equilibrium point $E(\lambda, k\lambda^2)$ when $\lambda < 0$, or $E(\lambda, \lambda^2 - \frac{1}{3}\lambda^3)$ when $\lambda \geqslant 0$.

2.2.1. The stability of the equilibrium point of system (2.6)

Theorem 2.3. *The stability of the equilibrium point E of system* (2.6) *is shown as follows.*

(1) *If $\lambda < -\frac{\sqrt{\varepsilon}}{k}$, then E is a stable node.*

(2) *If $\lambda = -\frac{\sqrt{\varepsilon}}{k}$, then E is a stable degenerate node.*

(3) *If $-\frac{\sqrt{\varepsilon}}{k} < \lambda < 0$, then E is a stable focus.*

(4) *If $\lambda = 0$, then E is a stable focus in the left half-plane and a stable first-order focus in the right half-plane.*

(5) *If $\lambda > 0$, the stability of E is consistent with system* (2.1).

Proof. For $\lambda < 0$, the Jacobian matrix of system (2.6) at equilibrium point E is $\begin{pmatrix} 2k\lambda & -1 \\ \varepsilon & 0 \end{pmatrix}$ with its eigenvalues $k\lambda \pm \sqrt{k^2\lambda^2 - \varepsilon}$. Conclusions come from Theorem 2.1. $\qquad\square$

2.2.2. Limit cycles of system (2.6)

Theorem 2.4. *There exists $\varepsilon_0 > 0$ such that for $0 < \varepsilon \leqslant \varepsilon_0$, the following conclusions hold for system* (2.6):

(1) *when $\lambda \leqslant 0$ or $\lambda \geqslant 2$, there is no limit cycle;*

(2) *when $0 < \lambda < 2$, there exists a unique stable limit cycle.*

Proof. When $0 < \lambda < 2$, the equilibrium point $E(\lambda, \lambda^2 - \frac{1}{3}\lambda^3)$ lies within the region M. By following the construction of the boundary curve in Theorem 2.2, we can demonstrate that system (2.6) has at least one limit cycle using the Poincaré-Bendixon theorem. Moreover, the stability of the limit cycle can be proved in two cases.

   Case 1: Assume that the limit cycle is located in region $L \cup M$ or $L \cup M \cup R$. When ε is sufficiently small, we calculate:

$$
\begin{aligned}
&\int_0^{T_1} \left(\frac{\partial P}{\partial x} + \frac{\partial Q}{\partial y} \right) dt + \int_{T_1}^{T_1+T_2} \left(\frac{\partial \tilde{P}}{\partial x} + \frac{\partial \tilde{Q}}{\partial y} \right) dt \\
&= \int_0^{T_1} 2kx\,dt + \int_O \frac{2x - x^2}{\varepsilon(x - \lambda)} dy < 0.
\end{aligned}
\tag{2.7}
$$

Thus, the limit cycle is stable and unique.

Case 2: Assume that the limit cycle is located in region $M \cup R$, and its stability has already been proven in Theorem 2.2.

If $\lambda \leqslant 0$ or $\lambda \geqslant 2$, and system (2.6) possesses a limit cycle, equation (2.7) implies that the limit cycle is both unique and stable. However, this contradicts the stability of the equilibrium point. $\square$

Remark 2.2. The limit cycle of system (2.6) does not lie within a single region.

3. The common features of two systems

3.1. Influence of ε

We define symbols as follows:

$$S_l^1 = \{(x, F_1(x)) : x < 0\}, \quad S_m = \{(x, F_1(x)) : 0 < x < x_M\},$$
$$S_l^2 = \{(x, F_2(x)) : x < 0\}, \quad S_r = \{(x, F_1(x)) : x > x_M\},$$

where x_M is the maximum point of $F_1(x)$ for $x > 0$, and y_M is the corresponding maximum value. Let $(x_r, 0)$ be the intersection point of the x-axis and S_r, and $\left(x_l^1, y_M\right)$ be the intersection point of the line $y = y_M$ and S_l^1. The singular orbit $\Gamma_1 = l_1 \cup l_2 \cup l_3 \cup l_4$, where

$$l_1 = \{(x, y) : y = F_1(x), x_l \leqslant x \leqslant 0\}, \qquad l_2 = \{(x, 0) : 0 \leqslant x \leqslant x_r\},$$
$$l_3 = \{(x, y) : y = F_1(x), x_M \leqslant x \leqslant x_r\}, \quad l_4 = \{(x, y_M) : x_l \leqslant x \leqslant x_M\}.$$

Let U be a tubular neighborhood of Γ_1. Then, we have the following result. The idea used here is inspired in [14].

Theorem 3.1. *For $0 < \lambda < 2$, system (2.1) has a unique strongly attracting limit cycle $\Gamma_\varepsilon^1 \subset U$ for sufficiently small ε, i.e., its Floquet exponent is bounded above by $-K/\varepsilon$, where K is a positive constant. As $\varepsilon \to 0$, the limit cycle Γ_ε^1 approaches the singular orbit Γ_1 in the Hausdorff distance.*

Proof. According to Fenichel's theory, there exists slow manifolds $S_{l,\varepsilon}$ and $S_{r,\varepsilon}$ perturbed by S_l and S_r respectively. Analysis of the extension of turning point shows that $S_{l,\varepsilon}$ and $S_{r,\varepsilon}$ pass through the vicinity of turning point and arriving the neighborhood of S_r and S_l, respectively. Let Δ be a transverse line segment on l_1, $\pi : \Delta \to \Delta$ be the return map. From the conclusions of Fenichel's theory, it is known that when ε is sufficiently small, π is a contraction map with a contraction rate bounded by $e^{-K/\varepsilon}$, where K is a positive constant. The following analysis is consistent with the analysis of Theorem 2.1 in [14]. $\square$

Let $\left(x_l^2, y_M\right)$ be the intersection point of the line $y = y_M$ and S_l^2. The singular orbit $\Gamma_2 = l_5 \cup l_2 \cup l_3 \cup l_6$, where $l_5 = \{(x, y) : y = F_2(x), x_l \leqslant x \leqslant 0\}$ and $l_6 = \left\{(x, y_M) : x_l^2 \leqslant x \leqslant x_M\right\}$. Let U be a tubular neighborhood of Γ_2. Similarly, we have

Theorem 3.2. *For $0 < \lambda < 2$, system (2.6) has a unique strongly attracting limit cycle $\Gamma_\varepsilon^2 \subset U$ for sufficiently small ε, i.e., its Floquet exponent is bounded above by $-K/\varepsilon$, where K is a positive constant. As $\varepsilon \to 0$, the limit cycle Γ_ε^2 approaches the singular orbit Γ_2 in the Hausdorff distance.*
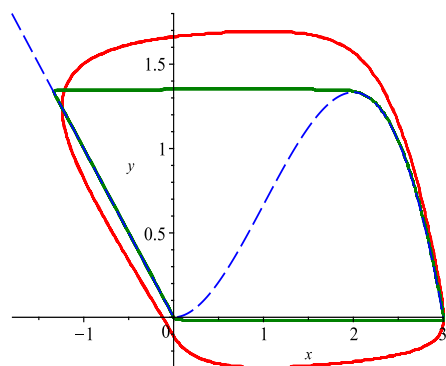
Figure 3. Relaxation oscillation of system (2.1)
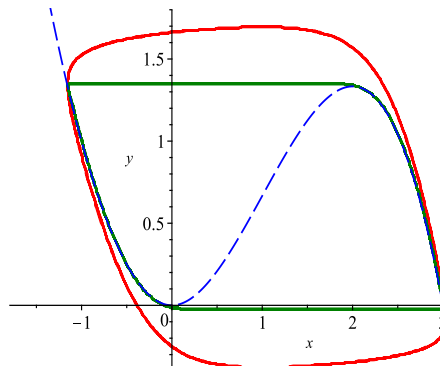
Figure 4. Relaxation oscillation of system (2.6)

Figures 3 and 4 illustrate the scenario when $k = 1$ and $\lambda = 1$ in two different systems. The red and green curves in the figures correspond to the cases of $\varepsilon = 0.1$ and $\varepsilon = 0.001$, respectively.

3.2. Influence of k

Next, we will examine how the value of k affects the position of the limit cycle. This conclusion applies to system (2.1) or (2.6).
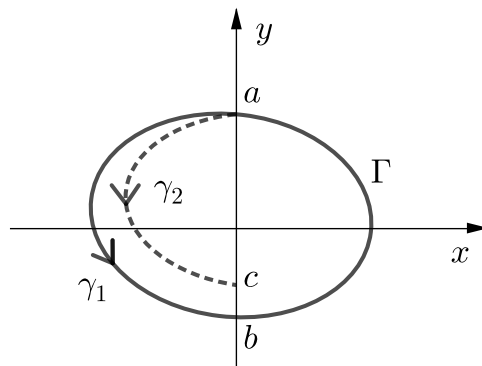
Figure 5. Trajectories in shadow and real system

Theorem 3.3. *When $0 < \lambda < 2$ and $0 < \varepsilon \ll 1$, the larger the value of k is, the smaller the limit cycle becomes, and the limit cycles with larger k values are surrounded by those with smaller k values.*

Proof. Let us designate the system with the larger k value as the shadow system and the system with the smaller k value as the real system. We can denote the limit cycle of the shadow system as Γ, and the intersection point of Γ with the positive y-axis as a, and the intersection point of Γ with the negative y-axis as b. Let γ_1 be the segment of γ_1 that extends from point a to point b. By applying the shadowing lemma, we can conclude that there exists a segment γ_2 that extends from point a to a point c on the negative y-axis of the shadow system. This segment γ_2 is

surrounded by γ_1 in the left half-plane, and we know that $0 > c > b$, as illustrated in Figure 5. This result can be derived from the Poincaré-Bendixon theorem.   □
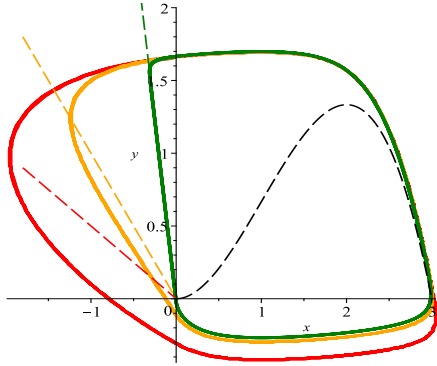
Figure 6. Limit cycles in system (2.1)   **Figure 7.** Limit cycles in system (2.6)
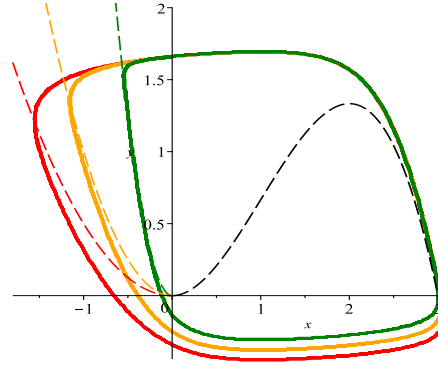
Figures 6 and 7 depict the scenarios for $\varepsilon = 0.1$ and $\lambda = 1$ in systems (2.1) and (2.6), respectively. The green, orange, and red curves correspond to the cases where $k = 0.5, k = 1$, and $k = 5$, respectively.

3.3. Influence of λ

3.3.1. Canard explosion in system (2.1)

In this subsection, we obtain a sufficient and necessary condition for the existence of Maximal canard in system (2.1) through the blow-up method. We remark that the turning point $(0,0)$ is a canard point of right-half system (2.1).

System (2.1) has a virtual equilibrium point $(\lambda, -k\lambda)$ for $\lambda \geqslant 0$. It has two invariant straight lines passing through the virtual equilibrium point in the left half-plane, i.e.

$$l_{\pm}: \quad y + k\lambda = \frac{-k \pm \sqrt{k^2 - 4\varepsilon}}{2}(x - \lambda), \quad x \leqslant 0.$$

Actually, l_- is the slow manifold $S_{a,\varepsilon}$ perturbed by $S_a = \{(x,y)|y = -kx, x \leqslant 0\}$. We are interested in the maximal canard, i.e., slow manifold $S_{a,\varepsilon}$ extends to slow manifold $S_{r,\varepsilon}$. The dynamics of $S_{r,\varepsilon}$ has been studied in [16] comprehensively, therefore we only need to analyze $S_{a,\varepsilon}$. Define a blow-up transformation in K_2 as follows:

$$x = r_2 x_2, \quad y = r_2^2 y_2, \quad \varepsilon = r_2^2, \quad \lambda = r_2 \lambda_2.$$

Mapping $S_{a,\varepsilon}$ to chart K_2 yields the equation

$$r_2 y_2 + k\lambda_2 = \frac{-k - \sqrt{k^2 - 4r_2^2}}{2}(x_2 - \lambda_2), \quad r_2 > 0.$$

The coordinates of its intersection with the hyperplane $x_2 = 0$ is

$$(0, \frac{-k + \sqrt{k^2 - 4r_2^2}}{2r_2}\lambda_2, r_2, \lambda_2).$$

It follows that

$$\frac{-k + \sqrt{k^2 - 4r_2^2}}{2r_2}\lambda_2 \leqslant 0, \quad \lambda_2 > 0, \quad 0 < r_2 \ll 1.$$

Consider the function $H(x_2, y_2) = \frac{1}{2}e^{-2y_2}(y_2 - x_2^2 + \frac{1}{2})$, which satisfies

$$\frac{\partial H}{\partial y_2}(0, y_2) \neq 0, \quad y_2 < 0.$$

Define $y_{a,2}(0)(y_{r,2}(0))$ as the y_2 component of the coordinates of the intersection of $S_{a,\varepsilon}(S_{r,\varepsilon})$ and the hyperplane $x_2 = 0$, then the distance function $y_{a,2}(0) - y_{r,2}(0)$ can be estimated by the function

$$D_c(r_2, \lambda_2) := H(0, y_{a,2}(0)) - H(0, y_{r,2}(0))$$

equivalently. Using conclusion (3.25) in [16] we obtain that

$$H(0, y_{r,2}(0)) = \frac{\sqrt{2\pi}e}{32}r_2 - \frac{\sqrt{2\pi}e}{4}\lambda_2 + O(2).$$

Substituting $(0, y_{a,2}(0))$ into H, we obtain

$$H(0, y_{a,2}(0)) = \frac{1}{2}e^{-\frac{-k+\sqrt{k^2-4r_2^2}}{r_2}\lambda_2}\left(\frac{-k + \sqrt{k^2 - 4r_2^2}}{2r_2}\lambda_2 + \frac{1}{2}\right).$$

Combining the above analysis, we draw the following conclusions.

Theorem 3.4. *System* (2.1) *has a maximal canard if and only if* $D_c(r_2, \lambda_2) = 0$.
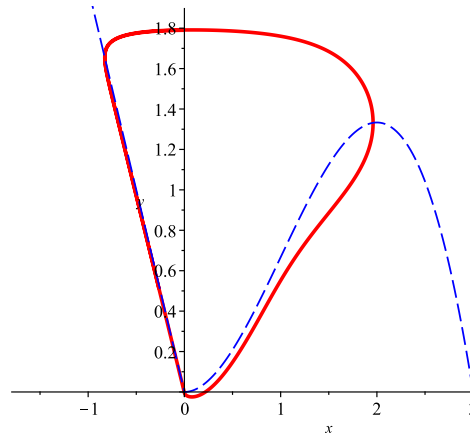
Figure 8. maximal canard in case $\varepsilon = 0.1$, $k = 2$, $\lambda = 0.078004$

3.3.2. Canard explosion in system (2.6)

In this subsection, we will show a canard explosion in system (2.6) for $k = 1$, i.e.,

$$\begin{aligned} x' &= -y + F(x), \\ y' &= \varepsilon(x - \lambda), \end{aligned} \quad F(x) = \begin{cases} g(x) = x^2, & x < 0, \\ f(x) = x^2 - \frac{1}{3}x^3, & x \geqslant 0. \end{cases} \quad (3.1)$$

Lemma 3.1 (Lemma 3.2 [15]). *Suppose that $\phi(x), p(x) \in C^\infty[a, b]$ satisfy the following conditions:*

(i) for any $n \geqslant 0$, $\phi(x)e^{np(x)}$ is integrable on $[a, b]$;

(ii) the function $p(x)$ has a unique maximum point at $x = \xi$, where $\xi = a$ (or b), and there exists an even integer $m \geqslant 2$ such that

$$p'(\xi) = p''(\xi) = \cdots = p^{(m-1)}(\xi) = 0, \quad p^{(m)}(\xi) < 0.$$

Then, the following estimate holds as $n \to \infty$:

$$\int_a^b \phi(x)e^{np(x)}dx = \frac{1}{m}\left(\frac{-m!}{np^{(m)}(\xi)}\right)^{\frac{1}{m}}e^{np(\xi)}\left(\sum_{i=0}^m \frac{\phi^i(\xi)}{i!}\left(\frac{-m!}{np^{(m)}(\xi)}\right)^{\frac{i}{m}}\Gamma\left(\frac{1+i}{m}\right) + o\left(\frac{1}{n}\right)\right),$$

where $\phi^{(0)}(\xi) = \phi(\xi)$, and $\Gamma(\alpha) = \int_0^\infty t^{\alpha-1}e^{-t}dt$ is the Gamma function.

Theorem 3.5. *The asymptotic expansion of the parameter for which a maximal canard exists in system (3.1) is $\lambda = \frac{1}{16}\varepsilon + O(\varepsilon^{3/2})$.*

Proof.   When $x \geqslant 0$, consider the right system

$$\begin{aligned} x' &= -y + f(x), \\ y' &= \varepsilon(x - \lambda). \end{aligned}$$

Let $y = f(x) + \frac{1}{x-2}\varepsilon + \varepsilon z$, then we have

$$\begin{aligned} \varepsilon\frac{dz}{dx} &= \frac{(x-2)^2 xz}{1 + (x-2)z} + \frac{\varepsilon}{(x-2)^2} + \frac{(x-2)\lambda}{1 + (x-2)z} \\ &= (x-2)^2 xz + G_+(x, z, \lambda, \varepsilon), \end{aligned}$$

where

$$G_+(x, z, \lambda, \varepsilon) = (x-2)\lambda + \frac{\varepsilon}{(x-2)^2} - \frac{(x-2)^3 xz^2}{1 + (x-2)z} - \frac{(x-2)^2 \lambda z}{1 + (x-2)z}.$$

When $x < 0$, consider the left system

$$\begin{aligned} x' &= -y + g(x), \\ y' &= \varepsilon(x - \lambda). \end{aligned}$$

Letting $y = g(x) - \frac{1}{2}\varepsilon + \varepsilon z$, we get

$$\varepsilon\frac{dz}{dx} = \frac{2(x-\lambda)}{1 - 2z} - 2x = 4xz + G_-(x, z, \lambda, \varepsilon),$$

where

$$G_-(x, z, \lambda, \varepsilon) = -2\lambda + \frac{4z(2xz - \lambda)}{1 - 2z}.$$

Therefore, the original system can be transformed to

$$\varepsilon\frac{dz}{dx} = \begin{cases} (x-2)^2 xz + G_+(x, z, \lambda, \varepsilon), & x \geqslant 0, \\ 4xz + G_-(x, z, \lambda, \varepsilon), & x < 0. \end{cases}$$

For $x \geqslant 0$, we obtain

$$z(x, \varepsilon) = z(q, \varepsilon) \exp\{\frac{Q_1(x) - Q_1(q)}{\varepsilon}\} - \frac{1}{\varepsilon} \int_x^q G_+(s, z(s), \lambda, \varepsilon) \exp\{\frac{Q_1(x) - Q_1(s)}{\varepsilon}\} ds,$$

where $0 < q < \frac{1}{2}$, $Q_1(x) = \int_0^x (s-2)^2 s \, ds = 2x^2 - \frac{4}{3}x^3 + \frac{1}{4}x^4$. It follows that

$$Q_1(0) = Q_1'(0) = 0, \quad Q_1''(0) = 4 > 0.$$

According to Lemma 3.1, we get

$$z_+(0, \varepsilon) = z_+(q, \varepsilon) \exp\{-\frac{Q_1(q)}{\varepsilon}\} - \frac{1}{\varepsilon} \int_0^q G_+(s, z(s), \lambda, \varepsilon) \exp\{-\frac{Q_1(s)}{\varepsilon}\} ds$$

$$= -\frac{1}{\varepsilon} \left(\sqrt{\frac{\pi\varepsilon}{8}}(-2\lambda + \frac{\varepsilon}{4} - \frac{4\lambda z(0)}{1 - 2z(0)}) + o(\varepsilon) \right)$$

and

$$z_-(0, \varepsilon) = z_-(-q, \varepsilon) \exp\{-\frac{Q_2(-q)}{\varepsilon}\} + \frac{1}{\varepsilon} \int_{-q}^0 G_-(s, z(s), \lambda, \varepsilon) \exp\{-\frac{Q_2(s)}{\varepsilon}\} ds$$

$$= \frac{1}{\varepsilon} \left(\sqrt{\frac{\pi\varepsilon}{8}}(-2\lambda - \frac{4\lambda z(0)}{1 - 2z(0)}) + o(\varepsilon) \right),$$

where $Q_2(x) = 2x^2$. By continuity, i.e., $z_-(0, \varepsilon) = z_+(0, \varepsilon)$, we get $\lambda = \frac{1}{16}\varepsilon + O(\varepsilon^{3/2})$. □

It follows from Theorem 3.5 that there exists a λ^* such that for $\lambda = \lambda^*$ system (3.1) has a maximal canard, where λ^* has the asymptotic expansion $\lambda^* = \frac{1}{16}\varepsilon + O(\varepsilon^{3/2})$. Take $\varepsilon = 0.01$. Then $\lambda^* \approx 0.000625 + O(\varepsilon^{3/2})$. Figure 9 shows the canard explosion by numerical simulation.
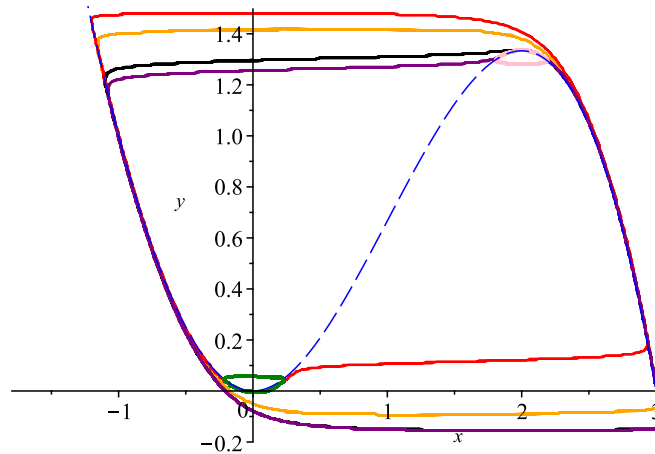
Figure 9. Canard explosion

The green orbit represents a canard without head for $\lambda = 0.000676$; the red orbit represents a canard with head for $\lambda = 0.000675$; the orange orbit represents relaxation oscillation for $\lambda = 1$; the black orbit represents relaxation oscillation for $\lambda = 1.98$; the purple orbit represents a canard with head for $\lambda = 1.9987$; and the pink orbit represents a canard without head for $\lambda = 1.99875$.

Remark 3.1. When $\lambda = 2$, the point $(2, 4/3)$ becomes a canard point in the right-half system. For further details, please refer to [16]. As a result, the shape of the limit cycle in system (3.1) can be predicted to vary with changes in the parameter λ.

4. Conclusions

In this paper, we have examined two types of piecewise smooth van der Pol equations, focusing on the existence, stability, and uniqueness of limit cycles. Our findings suggest that the qualitative conclusions of limit cycles should be comparable to those in the smooth situation. Furthermore, we have investigated the impact of parameters ε, k and λ on the limit cycle. Our results indicate that as ε approaches zero, the limit cycle tends towards the singular relaxation slow-fast orbit in the Hausdorff distance. Parameter k influences the size and position of the limit cycle, while the variation of parameter λ can lead to the canard explosion phenomenon, which is similar to the smooth case.

It is a pity that we have not yet been able to derive the asymptotic expression for the control parameter that allows for the existence of a canard in systems (2.1) or system (2.6) for $k \neq 1$. Nonetheless, the computer simulation results are consistent with our expectations, confirming the occurrence of canard explosion. This will be the primary focus of our future research.

References

[1] B. Van der Pol, *On relaxation-oscillations*, The London, Edinburgh, and Dublin Philosophical Magazine and Journal of Science, 1926, 2(11), 978–992.

[2] J. Llibre and X. Zhang, *Limit cycles of the classical Liénard differential systems: A survey on the Lins Neto, de Melo and Pugh's conjecture*, Expositiones Mathematicae, 2017, 35(3), 286-299.

[3] J. Llibre, E. Ponce and C. Valls, *Uniqueness and Non-uniqueness of Limit Cycles for Piecewise Linear Differential Systems with Three Zones and No Symmetry*, Journal of Nonlinear Science, 2015, 25, 861-887.

[4] Y. Xiong and C. Wang, *Limit cycle bifurcations of planar piecewise differential systems with three zones*, Nonlinear Analysis: Real World Applications, 2021, 61, 103333.

[5] Z. Yuan, A. Ke and M. Han, *On the number of limit cycles of a class of Liénard–Rayleigh oscillators*, Physica D: Nonlinear Phenomena, 2022, 438, 133366.

[6] S. Liu, X. Jin and Y. Xiong, *The number of limit cycles in a class of piecewise polynomial systems*, Journal of Nonlinear Modeling and Analysis, 2022, 4(2), 352-370.

[7] E. Benoit, J.F. Callot, F. Diener and M. Diener, *Chasse au canard*, Collectanea Mathematica, 1981, 32: 37-119.

[8] M. Desroches, E. Freire and S.J. Hogan, *Canards in piecewise-linear systems: explosions and super-explosions*, Proceedings of the Royal Society A: Mathematical, Physical and Engineering Sciences, 2013, 469(2154), 20120603.

[9] S. Fernández-García, M. Desroches, M. Krupa and A.E. Teruel, *Canard solutions in planar piecewise linear systems with three zones*, Dynamical Systems, 2016, 31(2), 173-197.

[10] S. Li and J. Llibre, *Canard limit cycles for piecewise linear Liénard systems with three zones*, International Journal of Bifurcation and Chaos, 2020, 30(15), 2050232.

[11] V. Carmona, S. Fernández-García and A.E. Teruel, *Birth, transition and maturation of canard cycles in a piecewise linear system with a flat slow manifold*, Physica D: Nonlinear Phenomena, 2023, 443, 133566.

[12] A. Roberts and P. Glendinning, *Canard-like phenomena in piecewise-smooth Van der Pol systems*, Chaos: An Interdisciplinary Journal of Nonlinear Science, 2014, 24(2), 023138.

[13] A. Roberts, *Canard explosion and relaxation oscillation in planar, piecewise-smooth continuous systems*, SIAM Journal on Applied Dynamical Systems, 2016, 15(1), 609-624.

[14] M. Krupa and P. Szmolyan, *Relaxation Oscillation and Canard Explosion*, Journal of Differential Equations, 2001, 174(2), 312-368.

[15] F. Xie, M. Han and W. Zhang, *The persistence of canards in 3-D singularly perturbed systems with two fast variables*, Asymptotic Analysis, 2006, 47, 95-106.

[16] M. Krupa and P. Szmolyan, *Extending geometric singular perturbation theory to nonhyperbolic points-fold and canard points in two dimensions*, SIAM Journal on Mathematical Analysis, 2001, 33(2), 286-314.